DOI: 10.13009/EUCASS2025-434
11TH EUROPEAN CONFERENCE FOR AERONAUTICS AND SPACE SCIENCES (EUCASS)

Investigation of combustion inhibitors to suppress pressure increase rate during solid motor ignition

Yasuhiro FUKUDA, Mano TAKESHI*, Yoshiki MATSUURA*, Atsushi TAKATA*,*
Shunsuke TAKAYAMA and Shinichiro TOKUDOME***
** IHI Aerospace Co., Ltd.*
900 Fujiki, Tomioka, Gunma 370-2398, Japan
*** Japan Aerospace Exploration Agency*
3-1-1 Yoshinodai, Chuo-ku, Sagamihara, Kanagawa 252-5210, Japan
yasuhiro-fukuda@iac.ihi.co.jp

Abstract
To operate SRMs in deep space, addressing challenges like the structural integrity of solid propellants in low-temperature environments is crucial. Strain strength of solid propellant decreases in low-temperature environments and high-strain-rate conditions, risking failure due to rapid pressure increase during ignition. This study investigates suppressing pressure increase rate by applying a combustion inhibitor to the initial burning surface. Appropriate inhibitor thickness and applicability were evaluated, confirming that uniform thickness is achievable through double-layer coatings. Small-scale motor tests demonstrated that the inhibitor effectively mitigates the initial pressure increase rate during combustion in low-temperature environments, providing a viable solution to enhance SRM performance in deep space exploration.

1. Introduction

Jupiter, Saturn, and the major icy satellites of Uranus are considered critical targets in the space exploration programs of various national space research agencies due to their numerous unknowns [1]. In contrast, Japan's deep space exploration strategy has predominantly focused on round-trip missions to small celestial bodies or flybys of large celestial bodies. This strategic choice is largely driven by a technical constraint: the absence of a stable and long-term power supply system required for Japan's deep space missions. Globally, radioisotope thermoelectric generators (RTGs) are extensively utilized in deep space exploration, enabling spacecraft to maintain a stable power supply even in environments with limited solar energy. However, Japan commenced research and development on RTGs in 2024, and there is no operational track record yet. As a result, solar power remains the only available power supply method for Japan. In deep space, however, the energy density of sunlight decreases significantly, resulting in a severely limited power generation efficiency. Consequently, this imposes substantial limitations on exploration strategies and mission designs.

In the context of the exploration of Jupiter and its moons considered in this study, the utilization of gravity assist maneuvers involving celestial bodies such as Earth, Venus, and Mars is essential. Gravity assist serves as an efficient method for increasing spacecraft velocity and plays a critical role in enhancing the energy required to reach the Jovian system. Furthermore, after the spacecraft reaches the Jovian system, a substantial deceleration (ΔV) is required to significantly slow down the previously accelerating spacecraft and enable its insertion into the orbit of the target celestial body for scientific exploration. From this standpoint, while electric propulsion systems offer advantages such as high specific impulse and superior fuel efficiency, their low thrust and the extended duration required for acceleration render them unsuitable for the rapid deceleration envisioned during orbital insertion in this study. Conversely, chemical propulsion systems, capable of delivering high thrust instantaneously, represent a more effective solution for achieving the rapid deceleration required for orbital insertion as anticipated in this study. In particular, solid propulsion systems, with their ability to generate high thrust in a short period of time, offer significant advantages for the mission considered in this paper, as they enable the rapid insertion of spacecraft into the target orbit [2].

Moreover, solid propulsion systems provide critical benefits in terms of thermal management. Liquid propulsion systems require complex insulation and heating systems to prevent fuel freezing. In the extreme cold environment of deep space, these heating systems, along with the solar array paddles required to power them, must be significantly enlarged. In contrast, solid propulsion systems, utilizing solid-state fuel, enable controlled operation at lower temperature compared to liquid propulsion systems, thereby reducing the power consumption required for temperature maintenance. This not only decreases the overall spacecraft weight and cost but also frees up power for scientific observations during the mission by removing the need for thermal insulation.

DOI: 10.13009/EUCASS2025-434

Given this context, solid rocket motors (SRMs) are considered highly effective for deep space exploration due to their ability to efficiently generate large ΔV and their ease of storage in low-temperature environments. However, SRMs also present certain unique challenges. The solid propellant used in SRMs can be designed to meet low temperature requirements from the perspective of material properties, but operational challenges arise during their application. Specifically, it is necessary to ensure that the solid propellant does not fail under the rapid stress changes induced by the pressure increase during ignition, especially in low-temperature environments. To address this issue, this study experimentally investigates an inhibitor application method to suppress the internal pressure increase rate and evaluates its effectiveness.

2. Challenges in Applying SRMs and Research Approach

To identify the challenges in applying SRMs to deep space exploration, the temperature conditions considered in this study are defined first. In the space environment, the temperature of the exploration stage is determined by the balance between the solar heat absorbed by the stage and the heat radiated from the stage into deep space. Regarding the temperature upon reaching the Jovian system, previous studies have conducted thermal analyses, which estimate that, without additional thermal control systems, the temperature of a metal motor case with a chromium-plated surface would be approximately -45°C in the Jovian system. And considering a margin, the target temperature is set to -50°C [3]. Therefore, this study aims to design SRMs that can function reliably in a low-temperature environment of -50°C.

One of the major challenges in operating SRMs under such low temperature conditions is ensuring the structural integrity of the solid propellant. Composite propellants, widely used in space SRMs, are viscoelastic materials composed of rubber binders, oxidizers, and metal particles. Their stiffness and strength depend on the strain rate, which indicates the amount of deformation per unit time and serves as an index of how quickly the propellant reacts to external loads. At higher strain rates (i.e., rapid deformation), viscoelastic materials like propellants exhibit increased stiffness but face a heightened risk of brittle fracture. Furthermore, these properties are significantly affected by temperature; at higher temperatures, the propellant behaves similarly to lower strain rates, while at lower temperatures, it behaves similarly to higher strain rates. (The parameter that expresses this time-temperature correlation is called the shift factor, aT.) Consequently, in low-temperature environments, the viscous component of viscoelasticity becomes insufficient, making brittleness more pronounced. When rapid pressure increases occur during ignition in such environments, the propellant is at a higher risk of fracture. In particular, the inner surface of the propellant bore forms a high tensile stress field due to combustion pressure, increasing the likelihood of fracture initiation at this location. Therefore, measures to prevent fractures on the inner bore surface are essential.

Specific measures to prevent fractures can be summarized as follows:

A. Improving the strain strength of the propellant
B. Suppressing the amount of deformation (strain)
C. Suppressing the rate of pressure increase (strain rate)

Measures A and B are aimed at enhancing strength or suppressing stress and strain, and these methods have been widely implemented in conventional SRM designs. Additionally, measure C, which focuses on suppressing the pressure increase rate, is a method that directly mitigates loading conditions. By suppressing the pressure increase rate, it allows for more time to accommodate the stress, enabling the SRM to operate within a range where the propellant's strain strength is higher. This approach is considered an effective complementary method to address the reduction in strain strength.

The approach focused on in this study is the application of an inhibitor coating method to the inner bore surface of the propellant. In this method, a combustion suppressant (inhibitor) is applied to the inner bore surface of the main motor propellant. During ignition, the inhibitor begins to burn gradually while undergoing thermal decomposition, thereby suppressing the internal pressure increase rate. The effectiveness of this method has been demonstrated in proof-of-concept experiments using small-scale motors [4]. Therefore, although this approach involves numerous research challenges, such as establishing manufacturability, reproducibility, and control methods for full-scale applications, it holds the potential to achieve reliable internal pressure control. However, prior studies have been limited to testing under ambient temperature conditions, and its performance in a low-temperature environments remains unverified.

To address this gap, this study adopts the inhibitor coating method as a measure to improve the structural integrity of solid propellants under low temperature conditions. As an initial step toward applying this method to full-scale systems, this research focuses on examining the inhibitor application process and conducting small-scale motor firing tests to evaluate the effectiveness of suppressing the internal pressure increase rate under low temperature conditions.

3. Examination of the Inhibitor

As mentioned before, the mechanism by which the inhibitor suppresses the rate of internal pressure increase involves initiating combustion gradually during ignition while undergoing thermal decomposition. To ensure the inhibitor

DOI: 10.13009/EUCASS2025-434

functions as intended, achieving appropriate film thickness and manufacturability is critical. To evaluate this, a trial was conducted, assuming the application to the inner surface of a full-scale motor.

3.1 Selection of Inhibitor Material

The inhibitor material was selected based on previous studies. The composition was determined by combining the fuel-binder of the solid propellant (HTPB rubber) with carbon black as a filler. This combination was chosen to maintain viscosity and ensure stable film thickness.

3.2 Evaluation of Inhibitor Application Workability

Two potential methods for applying the inhibitor were considered:
I. Bonding a pre-cured inhibitor to the propellant grain.
II. Directly applying the inhibitor onto the inner surface of the cured propellant and curing it.
As the complexity of the propellant grain geometry increases, method I becomes increasingly difficult to implement. Consequently, method II was selected for this trial. The manufacturing process for solid propellants involves filling uncured propellant into the casing space of the motor case and curing it in situ. During the filling process, a mandrel is placed inside the mold to form the inner bore, which is subsequently removed after curing. This process results in a smooth and glossy inner bore surface.
To simulate this application, the inhibitor was applied to a dummy propellant surface with a surface gloss equivalent to the actual release surface of the propellant. The inhibitor was applied at the levels indicated in Table 1, and the film thickness was measured on cross-sections of the specimens after curing. The application thickness was controlled by adjusting the amount of inhibitor applied per unit area.

Table 1: Coating Levels

Target Coating thickness	**Single Coating**	**Double Coating**
50 μm	n=1	n=1
100 μm	n=1	n=1
200 μm	n=1	n=1

The coating results are presented in Table 2 and Fig. 1. For target coating thicknesses of 50 μm and 100 μm, a single application caused the inhibitor to be repelled from the release surface, forming a mesh-like pattern. However, it was observed that applying the coating in double layers resulted in nearly uniform film thickness.
In contrast, for a target coating thickness of 200 μm, a single application also led to aggregation after coating, preventing the formation of a uniform surface. Even when the coating was applied in two layers, the excessive amount of coating material hindered the creation of a uniform surface. These observations indicate that a nearly uniform inhibitor coating can be achieved by applying the coating in double layers. Additionally, the optimal coating thickness per layer was found to be approximately 50 μm to 100 μm.

DOI: 10.13009/EUCASS2025-434

Table 2: Coating Results

Target thickness	**Single coating**	**Double coating**
50 μm	24～157 μm ave. 78 μm	23～240 μm ave. 100 μm
100 μm	36～303 μm ave. 150 μm	65～388 μm ave. 220 μm
200 μm	44～448 μm ave. 199 μm	107～940 μm ave. 612 μm

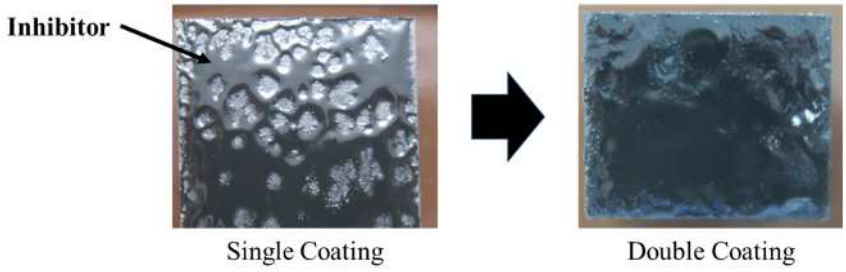

Figure 1: Coating Trial (Target: 100 μm per layer)

3.3 Evaluation of Inhibitor Retention under Simplified Heating

To evaluate the retention of the inhibitor under heating conditions, the inhibitor was applied to dummy propellant blocks at various film thickness levels, followed by simplified heating using a torch burner. The test conditions are summarized in Table 3, and the test setup is illustrated in Fig. 2.

Table 3: Test Conditions

Parameter	**Condition**
Gas Burner	Shinfuji Burner RZ-510
Heat Output	0.22 kW (190 kcal/h)
Flame Temperature	800-1300 ℃
Nozzle Diameter	11 mm
Air Setting	Maximum
Gas Flow Rate	Medium
Ignition Distance	15 mm
Burning Duration	10 sec
Inhibitor Coating	As shown in Table 1

DOI: 10.13009/EUCASS2025-434

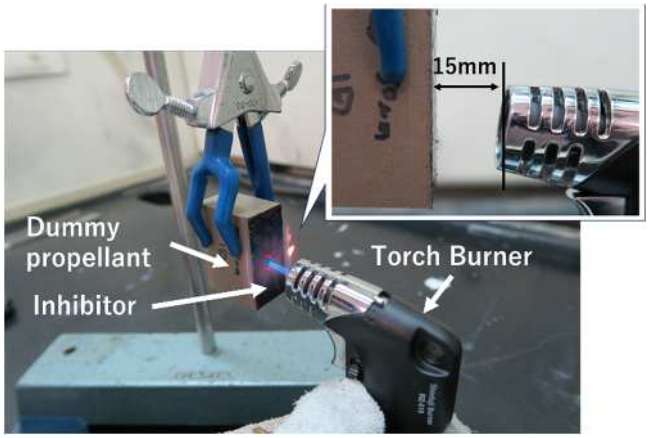

Figure 2: Simplified Heating of Inhibitor Using Torch Burner

The combustion results under each condition are shown in Fig.3.

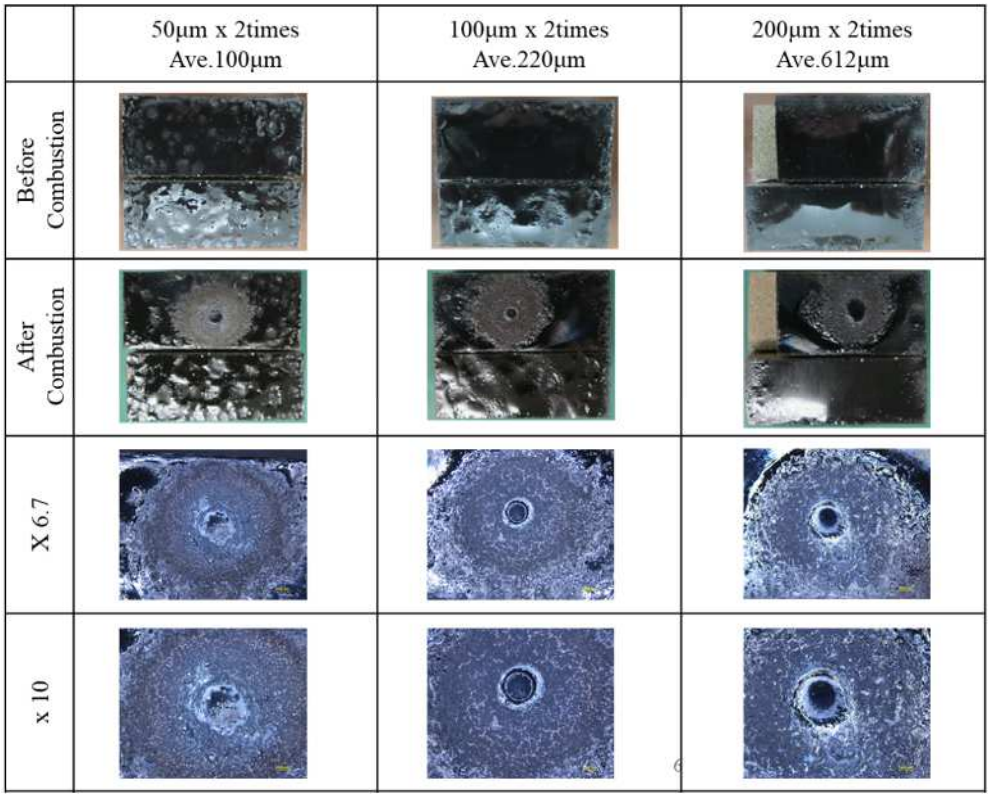

Figure 3: Simplified Heating Test Results

As a result, inhibitors with a thickness of less than approximately 200 μm disappeared, exposing the propellant surface. In contrast, when the coating thickness was set to approximately 600 μm, no exposure of the propellant was observed in the heated areas. Instead, the inhibitor remained as a layered structure with elasticity. This excessive residue suggests that the inhibitor may act not only as a combustion suppressant but also as a combustion restrictor, potentially disrupting the intended combustion pattern. The flame temperature of the torch burner reached a maximum of approximately 1300°C, which does not fully simulate the combustion gas temperature of 3351K during motor operation. However, based on these results, to ensure reliable exposure of the propellant surface during combustion, the maximum inhibitor coating thickness for the Φ110 motor firing test described in the next chapter was set to 200 μm.

DOI: 10.13009/EUCASS2025-434

4. Small-Scale Motor Firing Test

4.1 Experimental Setup

Based on the findings in Section 3, a firing test was conducted using a Φ110 motor to verify the initial pressure reduction performance of the inhibitor in both normal and low temperature environments.
The experimental setup is illustrated in Fig. 4, and the propellant mass used in the test is listed in Table 4. The composition of the propellant is provided in Table 5.

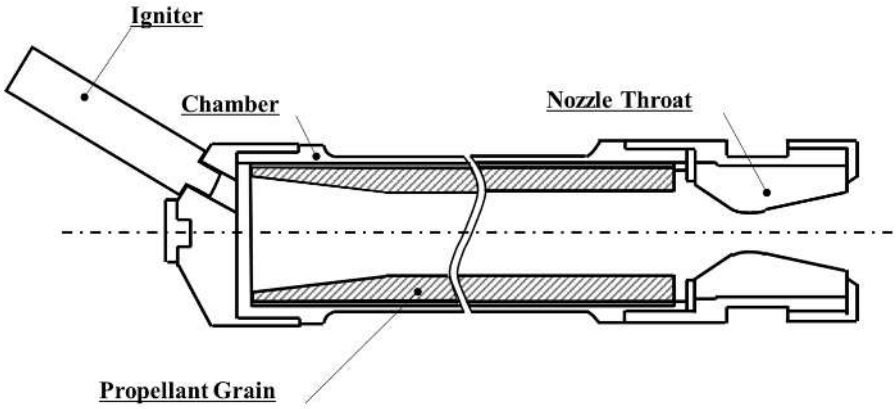

Fig.4 Overview of Experimental Setup

Table4 Propellant Mass

Test Condition	Propellant Mass [g]
20 ℃	3375.9
-50 ℃	3372.7

Table5 Composition of Properties

Component	HTPB-Binder	AP(NH_4ClO_4)	Al	Fe_2O_3
Composition [%]	14 %	68 %	18 %	0.01 %

To also verify the controllability of the inhibitor coating thickness, the test specimen was divided into three axial sections, with varying coating thicknesses applied to the inner surface of the propellant bore. The coating conditions are shown in Fig. 5. Based on the findings in Chapter 3, the coating thickness levels were set at two values: 100 μm and 200 μm.
For the 100 μm coating section, a single application of 50 μm was performed twice to achieve a total thickness of 100 μm. For the 200 μm coating section, the first 100 μm was applied using the same method as the 100 μm coating section, followed by an additional 100 μm coating, resulting in a total thickness of 200 μm through three applications. The inhibitor coating configuration is illustrated in Fig. 6.
The test conditions included two temperature settings: a low-temperature condition of -50 °C, which corresponds to the mission-expected low-temperature environments, and a normal temperature condition (20 ℃) added as a reference for comparison.

DOI: 10.13009/EUCASS2025-434

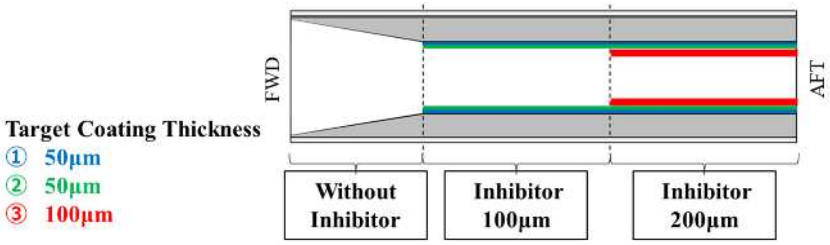

Fig.5 Coating Conditions of Inhibitor

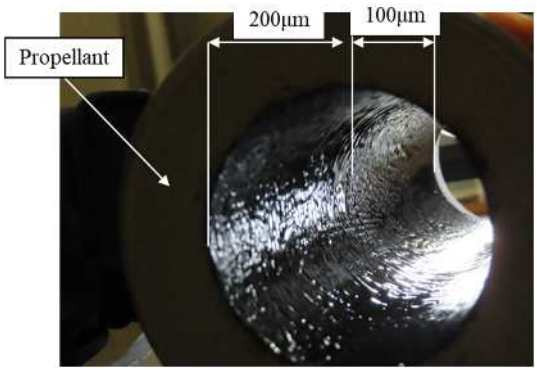

Fig.6 Inhibitor Coating State

4.2 Experimental Results

The motor chamber pressure-time histories under 20 °C and -50 °C conditions are shown in Fig. 7 and Fig. 8, respectively, with a comparison chart provided in Fig. 9. The results indicate no significant fluctuations in combustion pressure, confirming stable combustion.

When compared to the case without an inhibitor, the specimens with the inhibitor applied exhibited a slower initial pressure increase. Specifically, in terms of the time required to reach 75 % of P_{max}, the specimen without the inhibitor reached this level in 0.07 seconds, whereas the inhibitor-applied specimens required 0.2 seconds at 20 °C and 0.29 seconds at -50 °C. This indicates that the increase time with the inhibitor was more than three times longer. Additionally, a comparison of temperature conditions revealed that the increase time at -50 °C was approximately 0.08 seconds slower than at 20 °C.

The results of combustion characteristic analysis from pre-test combustion calculations are shown in Table 6, while the combustion characteristic analysis results based on the experimental data are presented in Table 7. A comparison between the experimental results and the predicted values from the pre-test analysis revealed that both the pressure impulse and characteristic exhaust velocity (C^*) were lower than predicted. Furthermore, these values were also lower compared to the data from specimens without the inhibitor.

DOI: 10.13009/EUCASS2025-434

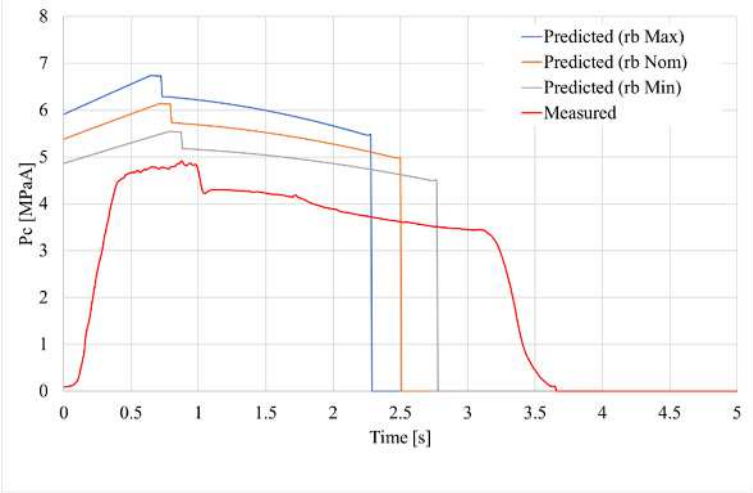

Fig.7 Combustion Pressure History (@20 ℃)

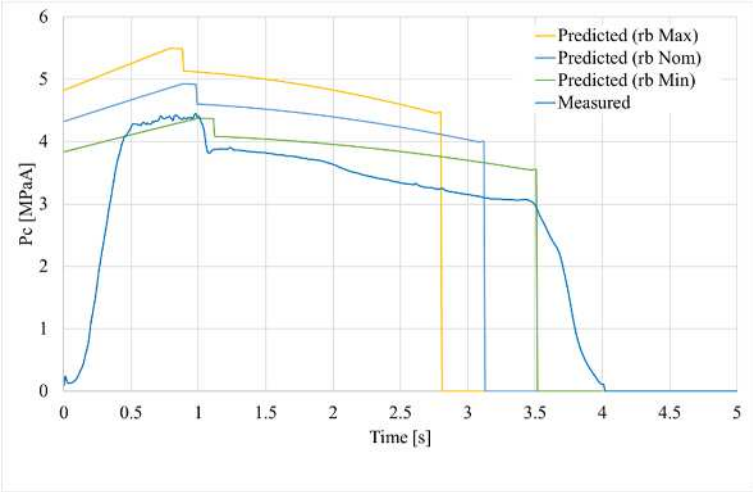

Fig.8 Combustion Pressure History (@-50 ℃)

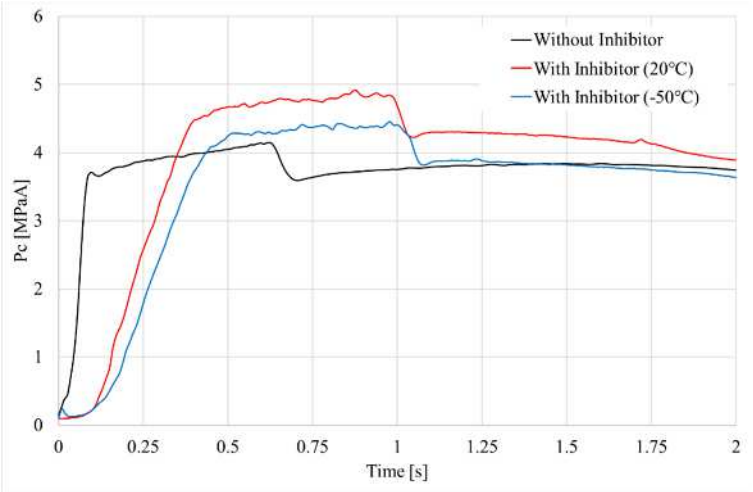

Fig.9 Comparison of Initial Combustion Pressure Histories

DOI: 10.13009/EUCASS2025-434

Table6 Predicted Combustion Analysis Values

Temperature [℃]	Burning Rate	Maximum Combustion Pressure P_{max} [MPa]	Combustion Duration t_b [s]	Pressure-Time Integral [MPa・s]	Characteristic exhaust velocity C* [m/s]
20	Max	6.74	2.28	13.90	1551.7
	Nom	6.13	2.50	13.87	
	Min	5.55	2.77	13.89	
-50	Max	5.50	2.80	13.91	
	Nom	4.93	3.12	13.90	
	Min	4.38	3.51	13.89	

Table7 Combustion Characteristics Analysis Results

	Throat Area A_t [mm^2]	Propellant Weight W_{pp} [kg]	Maximum Combustion Pressure P_{max} [MPaA]	Combustion Duration t_b [s]*1	Pressure-Time Integral [MPa・s]*2	Characteristic exhaust velocity C* [m/s]*3	75% P_{max} [MPaA]	Time to reach 75% P_{max} t [s] *4
With Inhibitor @20 ℃	402.9	3.4	4.9	3.5	12.7	1512.6	3.7	0.2
With Inhibitor @-50 ℃	402.7	3.4	4.4	3.9	12.6	1505.4	3.3	0.3
Ref. Without Inhibitor @20 ℃*5	368.4	3.4	4.2	4.2	14.2	1544.8	3.1	0.07

Notes
*1 The time from when the combustion pressure increases to 0.05 MPa until it decreases back to 0.05 MPa.
*2 Calculated over the entire combustion duration.
*3 $C^*=A_t \times \int Pdt / W_{pp}$
*4 The time from when the combustion pressure increases to 0.05 MPa until it reaches 75 % of P_{max}.
*5 The results of firing tests conducted in the past using a Φ110 motor. However, it should be noted that the propellant composition differs from that used in this study.

5. Discussion

This study evaluates the applicability of the inhibitor's pressure increase suppression effect, confirmed in the current experiment, to actual systems. In practical designs, the safety margin (M.S.) is assessed against the "strain at maximum nominal stress." However, in evaluating the equivalent strain rate, it is crucial to design the system such that the

DOI: 10.13009/EUCASS2025-434

material does not reach the region in which its properties drastically degrade (illustrated in Fig. 10). Here, the equivalent strain rate $\dot{\varepsilon}_r$ is adjusted using the shift factor (aT) to account for the viscoelastic material's temperature-time dependency, and it is expressed by the following equation:

$$\dot{\varepsilon}_r = aT \times \dot{\varepsilon} = aT \times {}^{\varepsilon}/_{t_r} \quad (1)$$

The strain induced on the inner bore surface of the propellant can be preliminarily estimated based on historical design data, considering the motor size and ignition pressure. The relationship between motor size (length/diameter = L/D) and the strain generated during ignition in previous Japanese motors is shown in Fig. 11. (Note: Since the rated pressure varies for each motor, the horizontal axis represents the product of L/D and the ignition evaluation pressure.)

To ensure sufficient ΔV for operations in the Jovian region, prior studies estimate the required motor size to correspond to approximately 2.5 tons of propellant. Based on data from motors of similar sizes, it is expected that about 4 % strain will occur. Aiming to halve this strain, the pressure increase time (t_r) is calculated using Equation (1), yielding an estimated requirement of approximately 5 seconds. However, in the current experiment, the pressure increase time was measured at 0.2 seconds, falling significantly short of the target.

Consequently, the current results indicate that improvements in propellant strain strength (as discussed in Section 2) and suppression of deformation (strain) are necessary for practical application. Additionally, this evaluation was conducted without fully optimizing the inhibitor's thickness or coating pattern, highlighting the need for further detailed studies moving forward.

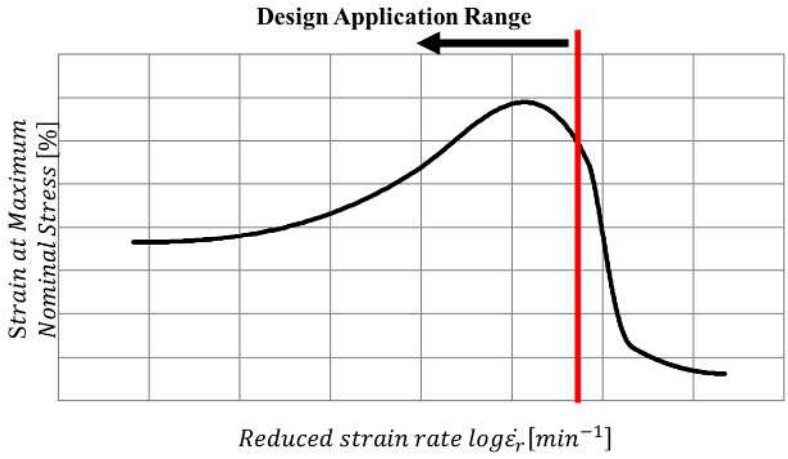

Fig.10 Relationship Between Equivalent Strain Rate and Strain at Maximum Nominal Stress

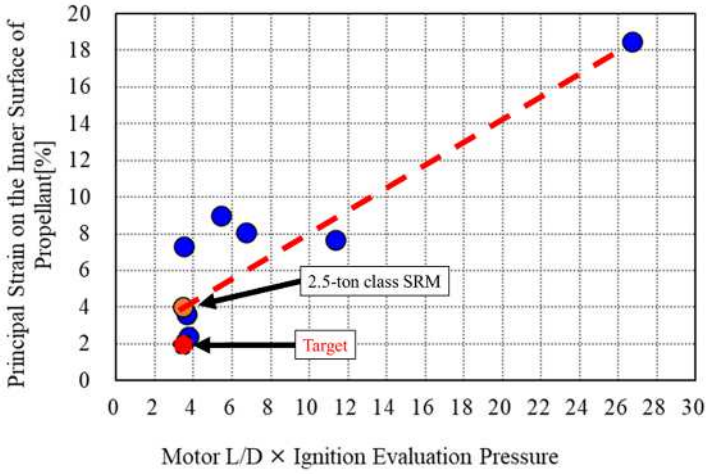

Fig.11 Relationship Between Motor Size and Strain Generated at Ignition in Previous Japanese Motors

For practical design applications, it is also necessary to establish predictive analytical methods. The suppression of the pressure increase rate by the inhibitor, based on its mechanism, can likely be reproduced in general solid motor combustion predictive analyses by setting a linear ignition delay from the forward to the aft section. In practice, it is essential to aim for the establishment of predictive methods through correlations with combustion patterns under various coating conditions.

DOI: 10.13009/EUCASS2025-434

Additionally, in the current experiment, the pressure-time integral was reduced by 10 % compared to the uncoated case. This significant reduction is strongly influenced by the inhibitor's effective time (pressure increase time), which is 0.2 seconds, accounting for approximately 5 % of the total combustion duration of 3.5 seconds. However, for a full-scale motor with a combustion time of approximately 100 seconds, the inhibitor's effective time would constitute only about 0.2 % of the total duration. Therefore, it is anticipated that the impact of the inhibitor on the pressure-time integral reduction would be minimal in actual systems. Plans are underway to validate this hypothesis through firing tests using scaled-up motors.

6. Conclusion

In this study, methods to suppress the pressure increase rate during ignition in low-temperature environments for SRM, assuming deep space exploration missions, were investigated. The following findings were obtained:

1. Fundamental data regarding inhibitor coating conditions, including film thickness and applicability, were acquired.
2. Small-scale motor firing tests confirmed the pressure increase suppression effect of the inhibitor coating during the initial ignition phase, demonstrating its applicability in low-temperature environments.

Based on the characteristics identified in this study, we aim to ensure the structural integrity of the propellant in low-temperature environments by combining it with conventional methods and advancing the design of SRMs suitable for deep space exploration.

Furthermore, to achieve this goal, we also plan to develop a predictive analytical model to evaluate the pressure increase rate mitigation effect of inhibitors. This model will be essential for designing combustion pressure profiles, including the pressure increase during ignition, which are critical for ensuring reliable SRM performance.

Additionally, we will continue to verify the practicality of manufacturing technologies for inhibitors capable of achieving the desired pressure increase rate during combustion. This will be done by progressively scaling up the motor size and conducting repeated tests.

7. Future Work

The following research tasks are outlined as future work. While this study focused on the structural integrity of propellants in low-temperature environments, additional evaluations of radiation resistance and high vacuum tolerance are necessary to realize the application of solid rocket motors for deep space exploration missions. These aspects will be addressed in future studies.

1. Confirmation of Reproducibility: Since the current tests were limited to a single trial, it is necessary to confirm the reproducibility of the results.
2. Validation with Large-Scale Motors: Investigate the feasibility of scaling up, including the applicability and uniformity of film thickness, and validate the effectiveness of the inhibitor under larger motor conditions.
3. Optimization of Combustion Control Technology: Further optimization of film thickness and application processes to maximize the combustion suppression characteristics of the inhibitor application method.
4. Establishment of Inhibitor Design Methods: Develop analytical prediction models to understand the relationship between inhibitor coating range/thickness and pressure increase suppression effects, thereby establishing combustion pattern design methods utilizing inhibitors.
5. Evaluation of Long-Term Durability: Assess the impact of the environmental conditions expected during a mission to the Jovian region (radiation, high vacuum, and temperature fluctuations) on the material properties of solid motor components.

References

[1] Y. Tsuda, T. Saiki, O. Mori, H. Kurokawa, Y. Shimaki, Y. Takao, Y. Maru, N. Bando, S. Tokudome, and N. Morishita, “Research Activities toward Next Next Generation Solar System Exploration (in Japanese), 2C01, The 67th Symposium on Space Science and Technology, Toyama, Japan, 2023, 17–20 October

[2] S. Tokudome, Takanao, Y. Saiki, Y. Tsuda, K. Sawada, N. Morishita, K. Kitagawa, K. Matsui, Y. Sakamoto, T. Matsunaga, K. Hori, S. Arakawa and Y. Matsuura; Deep-space Solid System for Orbiting Exploration of Large Gravity Bodies beyond the Asteroid Belt, IAC-24-C2.10.10

[3] K. Matsuhi, Y. Matsuura, S. Tokudome and K. Kitagawa, “Function Test of Experimental System to Obtain Laser Ignition Characteristics of Low-temperature Boron/Potassum Nitrate”, Journal of Evolving Space Activities Vol. 1, Arcticle No. 17, 2023.

[4] S. Tokudome, H. Tannno, N. Nakano, K. Kazuhige, I. Komai and M. Kohno, “NEW CONCEPTS OF SRM IGNITION SYSTEM”, ISTS 2000-a-28.